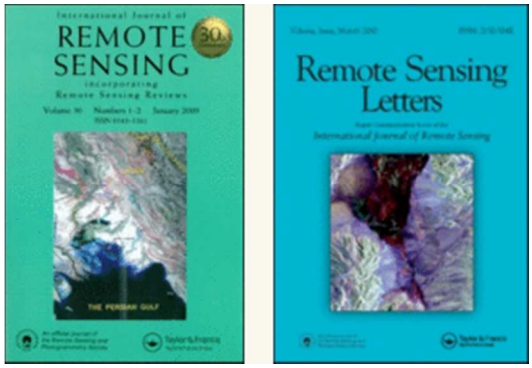

Comparison of vegetation phenology in the western U.S. determined from reflected GPS microwave signals and NDVI

Journal:	*International Journal of Remote Sensing*
Manuscript ID:	TRES-PAP-2013-0659
Manuscript Type:	IJRS Research Paper
Date Submitted by the Author:	05-Aug-2013
Complete List of Authors:	Evans, Sarah; University of Colorado Boulder, Geological Sciences small, eric; University of Colorado Boulder, Geological Sciences Larson, Kristine; University of Colorado Boulder, Aerospace Engineering Sciences
Keywords:	phenology, GPS, NDVI, reflectance
Keywords (user defined):	NMRI, start of season

Title: Comparison of vegetation phenology in the western U.S. determined from reflected GPS microwave signals and NDVI

Authors: *Evans, S.G.(1), Small, E.E.(1), Larson, K.M.(2)

1. Department of Geological Sciences, University of Colorado, Boulder

2. Department of Aerospace Engineering Sciences, University of Colorado, Boulder

Abstract

The Normalized Microwave Reflection Index (NMRI) is a measure of multipath scattering calculated daily from continuously-operating GPS sites. GPS satellites transmit L-band microwave signals, and thus NMRI is sensitive to the amount of water in vegetation, not plant greenness or dry biomass. The sensing footprint is approximately 0.1 km^2. NMRI exhibits clear seasonal variations that are linked to the changes in vegetation water content that accompany plant growth and senescence. In this paper, NMRI and NDVI are compared during the interval 2008-2012. The NMRI data are derived from 184 GPS sites in the western U.S. The NDVI data are averaged from the 250 m, 16-day pixels surrounding each GPS station. Amplitude of the annual growth cycle and the correlation between NMRI and NDVI are estimated, with and without lags. Phenology metrics are calculated from both indices, i.e. the start of the growing season, timing of peak growth, and season length.

NMRI and NDVI are correlated at most sites, but the degree of correlation varies regionally. Correlation is lowest in the California and coastal regions (R^2=0.26), where NDVI increases earlier in the spring than NMRI. It is highest for mountain and prairie sites (R^2=0.49). Allowing for a lag between NMRI and NDVI greatly increases the correlation. The lag that yields the greatest correlation is nearly 30 days for the California sites (R^2=0.52 with lag), but only 10 days for mountain and prairie sites (R^2=0.72 with lag). There are clear differences in

phenology metrics extracted from NMRI and NDVI that are consistent with the correlation-lag analysis. Using NMRI, there is a later start of season, later peak day of year, and shorter season length. The greatest differences are in California where NDVI start of season is nearly 60 days earlier than calculated from NMRI. These data suggest that greenup precedes increases in vegetation water content, with the duration of offset varying regionally. This study is the first to compare GPS-derived microwave reflectance data with NDVI at many sites, and highlights both opportunities and limitations offered by NMRI data.

1. Introduction

Vegetation state measurements are necessary for monitoring the phenology of ecosystem variables (Rondeaux et al., 1996; White et al., 2009; Jones et al., 2011), validating long-term land cover satellite estimates (Lu 2006; Hobbs, Yates, and Mooney 2007), and testing climate change and carbon cycle models (Cihlar et al., 1991; Sellers et al., 1992; Paruelo & Aguiar, 1993; Sellers et al., 1995; Nemani et al., 2003). With increasing temperatures and amplified drought conditions expected in the long term (Karl et al. 2012) it is necessary to understand how water is used by vegetation before characterizing climatic and soil-water interactions at regional and even global areas (Burke et al., 1991; Paruelo & Lauenroth, 1995; Rodriguez-Iturbe, 2000).

Phenology, the study of the timing of biological events, integrates climate-biosphere relationships and is used to evaluate the effects of climate change (Schwartz et al., 2006; Cleland et al., 2007). Understanding the timing, rate, and duration of vegetation growth is key in the study of global change and the carbon cycle. The timing of vegetation growth controls photosynthesis, carbon sequestration, and land–atmosphere water and energy exchange (Peñuelas, 2009; Morisette et al., 2009; Jones et al., 2011). Variations in seasonal onset of

vegetation growth have been documented at both the *in situ* measurement scale (Wolfe, Schwartz, and Lakso 2005) and the global satellite derived scale (Karl et al. 2012). With recent climate change, phenologists have noted earlier spring onsets and delays in the end of growing seasons (Parmesan 2007; Peñuelas 2009). In order to more fully characterize vegetation and how it is changing, we need to develop new methods to phenology metrics at appropriate spatial and temporal scales.

Normalized Difference Vegetation Index (NDVI), one of the most widely used vegetation remote sensing methods, is calculated as the difference between near-infrared (NIR) and visible (VIS) reflectance values normalized over the sum of the two (Eidenshink 1992):

$$\mathrm{NDVI} = \frac{(\mathrm{NIR} - \mathrm{VIS})}{(\mathrm{NIR} + \mathrm{VIS})}$$

Healthy green leaves have an internal mesophyll structure that reflects near-infrared radiation and also contains leaf chlorophyll to absorb red visible radiation (Wang et al., 2003). This makes NDVI a good indicator of the ability of plant matter to absorb photosynthetically active radiation, and therefore NDVI is often used to estimate green biomass or phytomass (Gamon et al. 2012; Al-Bakri and Taylor 2003; Holm 2003). NDVI is also used to estimate other vegetation properties, including leaf area index (Burke et al., 1991; Goetz, 1997), evapotranspiration (Cihlar, St-Laurent, and Dyer 1991), and primary productivity (Box, Holben, and Kalb 1989; Rodriguez-Iturbe 2000; Paruelo et al. 1997). For over 30 years, NDVI has been used to monitor the phenological state of vegetation from landscape to global scales (Tarpley et al., 1984; Running & Nemani, 1988).

While NDVI is useful for documenting greenup and seasonal fluctuations in vegetation activity, it has a variety of shortcomings, including: problems with background effects from soil (Paruelo et al. 1997; Montandon and Small 2008), atmospheric effects (Rondeaux et al., 1996;

Myneni & Williams, 1994), smoke and aerosol contamination (Jones et al., 2011), cloud cover (Champion and Guyot 1993), complex terrain (Box, Holben, and Kalb 1989), weather (Brakke, Kanemasu, and Steiner 1981), time of day (Kim, Jackson, and Bindlish 2012), and interruption of signals at high latitudes (Box, Holben, and Kalb 1989). Standard NDVI products derived from MODIS and other satellites have a repeat frequency of 8 or 16 days. Thus accurate derivation of phenology metrics, such as vegetation start of season, suffer from the coarse time step of NDVI (Fischer 1994). Additionally, NDVI has limited sensitivity to drought conditions due to its spatial compositing procedure which biases the high end of its spectral signature (Burke et al., 1991).

Other spectral vegetation indices such as Soil-Adjusted Vegetation Indices (SAVI) include soil-line parameters (Rondeaux, Steven, and Baret 1996). Compared to NDVI, SAVI considerably reduces influences from soil and surface roughness resulting in a lowered vegetation index signal (Huete 1988). Although SAVI reduces soil effects, it still yields imprecise vegetation estimates, particularly when there is limited vegetation cover (Rondeaux, Steven, and Baret 1996). SAVI is not as commonly used as NDVI. Normalized Difference Water Index (NDWI), another optical remote sensing method, utilizes a water absorption band at 1.24 μm. NDWI measures interactions between liquid water molecules in vegetation canopies and incoming solar radiation (Chen, Huang, and Jackson 2005). However, NDWI is not a better predictor of vegetation water content than NDVI, especially at sites with soil background reflectance effects (Gao 1996; Serrano, Filella, and Penuelas 2000; Chen, Huang, and Jackson 2005). Therefore, only NDVI will be addressed further in this paper.

Remote sensing with microwave radar has advantages in that it is not limited by cloud cover, weather, or time of day (Ulaby & Wilson, 1985). Passive microwave data have been used

to monitor plant phenology (e.g., Jones et al., 2011). Active microwave data may also be used to accurately determine vegetation water content and estimate biomass (Lu 2006; Kim, Jackson, and Bindlish 2012). Since the dielectric constant for water is an order of magnitude greater than for dry vegetation at microwave wavelengths (Schmugge 1978), changes in moisture content of vegetation can results in significant changes in microwave scattering coefficients (Brakke, Kanemasu, and Steiner 1981). Primary challenges when using microwave data for vegetation studies are integrating heterogeneous plant dielectric properties through the canopy layer (O'Neill et al. 1984) and removing the effects of soil moisture and surface roughness (De Roo et al., 2001; Ulaby & Wilson, 1985; Ulaby et al., 1984).

Global Positioning System-Interferometric Reflectometry (GPS-IR) is a bistatic, microwave radar remote sensing technique (Larson and Small, 2013). Previously it has shown potential for monitoring vegetation height and water content (Small, Larson, and Braun 2010). GPS satellites transmit at L-band (microwave bands at 1.22760 and 1.57542 GHz) which is similar to those used in active microwave radar applications. L-band signals have a higher correlation with vegetation water content than C-band signals (4 to 8 GHz) (Kim, Jackson, and Bindlish 2012), and thus one would expect GPS-IR to correlated with vegetation water content. Initial validation versus field measurements has shown this to be the case (Small, Larson, and Braun 2010; Small, Larson, and Smith, 2013). As NDVI measures greenness, the GPS data are complementary to NDVI products.

GPS-IR is sensitive to surface environmental conditions due to reflection effects (dielectric constants) of the surface and the signal propagation delay. Although designed to minimize reflection effects, geodetic GPS instruments can be used for GPS-IR (Larson et al. 2008). Using geodetic instruments means that tens of thousands of the GPS receivers operating

around the world are potentially usable for phenology studies. In this study GPS instruments operated by the EarthScope Plate Boundary Observatory (PBO) are used (Larson and Small, 2013). PBO sites are located in the western United States to measure deformation of the Pacific-North America plate boundary. For this reason the highest density of PBO sites is in California. Vegetation types at PBO sites are dominantly grass, woody savanna, and shrub. In this paper, we use the Normalized Microwave Reflection Index (NMRI), a measure of the intensity of GPS reflections. It is derived from standard GPS data (Larson and Small, 2013).

NMRI, and GPS-IR data in general, offers some unique benefits that are not provided by other techniques used for remote sensing of vegetation. The sensing footprint of GPS (~0.1 km^2) is smaller than that of spaced-derived remotely sensed products such as spectral vegetation indices (~0.6 km^2), but larger than that of *in situ* observations (e.g. clipping and drying, ~1 m^2). Additionally, GPS instruments can provide daily estimates of vegetation state, which is more frequent than provided by other sensors. The primary drawback of GPS-IR is that it can only be used where instruments have been deployed.

NMRI has been compared to vegetation parameters measured at agricultural and natural grassland sites and a small number of comparisons between NMRI and NDVI have been described (Small, Larson, and Braun, 2013). The purpose of this study is to compare NMRI and NDVI signals at hundreds of sites across the western U.S. The vegetation at these sites is typical of the non-forested ecosystems in the region. Climate varies greatly across the sites, depending upon latitude, elevation, and proximity to the coast. We derive NMRI and NDVI amplitude of the annual growth cycle, correlation between NMRI and NDVI signals, and phenology parameters. Phenology metrics include start of season day of year, season length, and peak day

of year of vegetation growth. Comparisons are completed at both the site level and at the regional scale.

2. Derivation of NMRI and NDVI metrics

We selected 184 sites from the PBO Network in the western United States (Figure 1). (Insert Figure 1 here) We picked sites in non-urbanized areas that were surrounded by the following land cover types: grass, shrub, savanna, or sparse vegetation, according to the MODIS MCD12Q1 500-m land cover product using the IGBP classification scheme (Loveland et al. 2000). PBO GPS installations are not located beneath forest canopies, as trees degrade estimates of position. However, there are GPS sites are in forested regions, with the antenna located in clearings ~100 m in diameter or larger. We attempted to exclude sites of this variety because NMRI and NDVI could potentially be sensing different vegetation: NMRI would be sensitive to the vegetation in the clearing, whereas NDVI would include effects from the surrounding forest. A subset of the sites we selected was affected by this problem (Section 4).

2.1 Data acquisition

2.1.1 NMRI

The default sampling interval for PBO sites is 15 seconds, and there are more than 30 GPS satellites transmitting continuously in ~12 hour orbits. In order to summarize the quality of the ranging observations, an average measurement noise statistic is recorded from each GPS site every day. These noise values are then normalized to remove first order terrain effects. A detailed derivation of NMRI can be found in Larson and Small (2013).

2.1.2 NDVI

We derive NDVI data from NASA's Moderate Resolution Imaging Spectroradiometer (MODIS), MOD13Q1, 250 meter pixel, 16-day composite products. Each NDVI data point is a

composite created using the Maximum Value Composite (MVC) technique. This technique is frequently performed on NDVI data to reduce both cloud contamination and data volume (Swets et al. 2001). Using the MVC technique, the highest NDVI values from daily images over 16-day periods are selected and reported (Holm 2003). For this study, we use NDVI data from the pixel that contains each GPS station (Holm 2003).

2.1.3 Precipitation and temperature

Mean annual precipitation (MAP, mm) and mean annual temperature (MAT, ºC) are extracted from hourly North America Land Data Assimilation System (NLDAS-2) modeled data at each site (Mitchell et al. 2003). Daily values are computed (maximum, minimum, and average) for each of these quantities. This data is interpolated to have 12 km spatial resolution and one hour temporal frequency (NLDAS; http://ldas.gsfc.nasa.gov/nldas/NLDAS2model.php).

2.2 Data cleaning

NDVI is minimally edited. Negative NDVI values and data on days that NLDAS data record snow events are removed. NLDAS snow events are identified when the temperature falls below 1 ºC and there is more than 2 mm of daily precipitation. Examples of NDVI time series are presented for site p041 in Colorado and for site p208 in California (Figure 2*a* and *e*). (Insert Figure 2 here). NMRI data are also removed on days when NLDAS indicates snow. In addition, NMRI data are removed on days when NLDAS indicated rainfall in excess of 10 mm (Figure 2*b* and *f*). We have found that rainfall of this magnitude yields NMRI outliers on the day of rainfall, most likely due to changes in reflectivity with precipitation (Larson and Small, 2013). Remaining outliers are removed using a centered, five day median filter (Figure 2*c* and *g*). Gaps are filled via linear interpolation for both NDVI (Figure 2*a* and *e*) and NMRI (Figure 2*d* and *h*). Phenology metrics are calculated using the gap-filled data.

2.3 Amplitude, correlation, and lag metric derivation

After NMRI and NDVI data cleaning, three metrics are derived on a site by site basis: amplitude of the annual growth cycle, correlation between NMRI and NDVI data, and correlation lag. We calculate amplitude for NMRI and NDVI for each site as the difference of the 95^{th} and 5^{th} percentile data values. This calculation is completed for each water year between 2008 and 2012 (Figure 2*b* and *f*, blue lines show 95^{th} and 5^{th} percentiles). Each water-year goes from day of year (doy) 275 of the previous year to doy 274 of the current year. One NMRI and NDVI amplitude value is calculated for each site by averaging the values from the five water years.

Correlation values are found by extracting NMRI data on days that also have NDVI data and computing a standard R^2 coefficient of determination statistic. We do not use gap-filled time series (e.g., Figure 2*a* and *c*) for this analysis. To take into account lag between NMRI and NDVI signals, NMRI points are extracted for days that have NDVI data plus a specified lag value (in days). R^2 correlation was computed for each lag amount. Lag was tested from zero to 45 days to determine the amount of lag necessary for maximum correlation. 180 sites had positive lag days; four sites had zero or negative lag days.

2.4 NMRI and NDVI seasonality metric derivation

Cleaned, gap-filled daily NMRI and NDVI time series were used to compute phenology metrics (e.g., Figure 2*a* and *e*). The NDVI data are only available as a 16 day composite, with anywhere between one and 31 days between sample points. Likewise, there were gaps in the daily NMRI data due to snow cover or rainfall. In order to overcome these problems and produce directly comparable data, the same method was used for both NMRI and NDVI phenology metrics. Two examples are shown in Figure 2: site p208 in California, which has a

large amplitude and low noise, and site p041 in Colorado, which has a smaller amplitude and noisier signal.

To make sure that linear interpolation of NDVI did not impact the comparison of NMRI and NDVI, we repeated all calculations as follows. A second NMRI time series was produced for each site using only the data from days which had NDVI data. Linear interpolation was then applied to this NMRI time series. All statistics were calculated using this second NMRI time series. Results were very similar to what is shown below. We chose to use the undecimated NMRI phenology results, as these are more true to the data.

NMRI phenology metrics are defined with a threshold method (Figure 2*d* and *h*, green line) that requires the data to remain above a fixed 25% of the seasonal amplitude for a minimum of 40 days (Jones et al., 2012). This threshold method was tested against a third derivative approach from an asymmetric Gaussian fitting routine in TIMESAT (Jönsson and Eklundh 2004). TIMESAT requires previous and following year data to pad the current year data. The threshold approach was not limited by padding, so we were able to compute metrics for five water-years, 2008-2012. Annual NDVI metrics are produced using an identical procedure.

Three phenology variables are considered: start of season (SOS), season length, and peak vegetation doy. The SOS or greenup date signifies the first pulse of greenness or increase in vegetation water content. SOS was determined to be when the NMRI or NDVI variable first crosses the 25% threshold (Figure 2*d* and *h*, green line). The magnitude of the 25% threshold changes from year to year, according to the NMRI or NDVI values during that year (e.g., Stein, 1999).

The start and end of season dates depend on the threshold chosen. In some studies, a 50% threshold has been used because the rate of change in greenness is greatest with this

threshold (De Beurs 2008). Here, we used a 25% threshold (Figure 2), more indicative of a first growth pulse (e.g., Jones et al., 2012). We also required that the index stay above this threshold for 40 consecutive days (Figure 2*d* and *h*, red dots), to exclude any short duration events not part of the annual growth cycle. Season length is computed as the time between SOS and end of season or senescence when the index falls below the 25% threshold. Peak vegetation doy is determined from the annual maximum of the NDVI or NMRI index.

2.4.1 Uncertainty and sensitivity to parameters

We did not include 11 sites (out of 184) in the phenology analysis because of challenges faced when applying the method described above. At these sites, the index did not exceed the 25% threshold for 40 continuous days in all five years. We altered the threshold percent and days above threshold but results were similar. Thus, we only present phenology metrics from 173 sites.

2.5 Regional Analysis

Clustering sites by region is useful for analyzing phenological responses at the ecosystem level (White, 2005; Hargrove & Hoffman, 1999). Our sample GPS sites span 25 North American level-III ecoregions as defined by the Commission for Environmental Cooperation (Omernik 1987; U.S. Environmental Protection Agency 2011). These subdivisions are made according to climate, hydrology, vegetation, wildlife, and land use/human activities (Wiken, Nava, and Jimen 2011). We grouped the sites into five regions: Mountain (n=25), Coast (n=14), Prairie (n=8), Desert (n=38), and Mediterranean California (n=99) (Figure 1). Some of the Mediterranean California sites are 'coastal' (see Figure 1 for details). Many of the stations (n=99) fall into Mediterranean California region, which include coastal sage, chaparral, and oak woodlands. The Mediterranean California sites have been subdivided into land types of

grassland (n=66) and shrub (n=33) based on evaluation of photographs and MODIS MCD12Q1 500-m land cover product using the IGBP classification scheme (Loveland et al. 2000). By clustering sites into land cover regions we highlight vegetation phenological responses to climate constraints and reduce the effects of spatial heterogeneity between sites.

3. Results

3.1 NMRI and NDVI amplitude

We compare the amplitude of NMRI and NDVI seasonal cycles in Figure 3. (Insert Figure 3 here). Each small point represents the five-year average from an individual site (2008-2012). As each index is normalized independently, the values are not expected to be equal. The amplitude of NMRI and NDVI are correlated across sites ($R^2 = 0.31$). To a first order, sites with the highest NDVI amplitude have the highest NMRI amplitude. These sites are primarily located in the Mediterranean California sites and mountain regions. The lowest NMRI and NDVI amplitudes are from desert sites. Others are intermediate. Few sites have low NDVI and high NMRI amplitude values. However, some sites do have high NDVI and low NMRI amplitude values, yielding the triangular pattern evident in Figure 3.

The region-average NMRI and NDVI amplitudes cluster around the total population mean (Table 1). (Insert Table 1 here). They show a similar pattern as the individual sites: Mediterranean California sites have the highest amplitudes (Figure 3). The region-averaged NMRI and NDVI amplitude values from the coast region are not consistent: this region has the lowest NMRI amplitudes and one of the highest NDVI values. This mismatch can also be seen for the individual coastal points. The likely source for this difference between NMRI and NDVI amplitudes from coastal sites is addressed in the discussion.

3.2 Correlation between NDVI and NMRI

The temporal fluctuations of NMRI and NDVI are generally correlated. However, the nature of the correlation varies from site to site. Examples of the correlation between NMRI and NDVI from three sites are presented in Figure 4. (Insert Figure 4 here). The sites differ in terms of climate and vegetation, and thus demonstrate the range of correlation patterns that exist. At site p041 in Marshall, Colorado the NDVI and NMRI data pairs are strongly correlated (R^2=0.65) (Figure 4). NDVI and NMRI increase together during the spring (March through May) and decrease in the summer (see Figure 2 for time series). The timing and extent of seasonal growth varies from year to year, but these changes are similar for both NMRI and NDVI. Prairie site p046 in Bonner, Montana has a lower correlation than p041 (R^2=0.54) because the springtime increases of NDVI and NMRI occur at different times (Figure 4, middle plot). NDVI increases in April and May while NMRI remains relatively constant. By early June, NMRI begins to increase more rapidly while NDVI remains nearly constant. For the remainder of the growing season, NMRI and NDVI covary.

A more extreme example of differences in the timing of NMRI and NDVI changes can be seen at site p208 in Williams, California (R^2=0.24) (Figure 4, and Figure 2 for time series). NDVI increases between January and March while NMRI remains constant. Then, NMRI increases during April and May while NDVI remains nearly constant. Both decrease together after senescence. Of the three example sites, this site has the lowest correlation value due to the marked hysteresis on the NMRI-NDVI plot.

The correlation between NMRI and NDVI varies greatly across the 184 sites, with R^2 values ranging from 0.00 to 0.78 (mean=0.31±0.2) (Table 1). The degree of correlation varies from region to region (Figure 5, blue bars). (Insert Figure 5 here). NMRI and NDVI covary most strongly in the mountain and prairie regions (R^2 is 0.46±0.2 and 0.49±0.1, respectively),

which include sites in Montana, northern Utah, Idaho, Colorado, Wyoming, and eastern Oregon. These sites have the greatest temperature limitations on vegetation. Sites in the precipitation-limited Mediterranean California region, for example site p208 (Figure 4), tend to have lower correlations ($R^2 = 0.26 \pm 0.2$). Within this region, shrub sites exhibit lower NMRI-NDVI correlation values than grasslands (Table 1). The lowest correlations are found in the coastal region, including sites in western Oregon and Washington (coast: $R^2 = 0.10 \pm 0.1$).

Allowing for a lag between NMRI and NDVI increases the correlation between the two indices at most of the sites. As shown in Figure 4, NDVI tends to increase earlier in the spring than NMRI, with the magnitude of the lag varying by site. We calculated the lag that yields the greatest correlation at each site individually. The average lag across the 184 sites is 21 days: NMRI changes occur approximately three weeks later than changes in NDVI. There are significant differences from region to region. On average, sites in the mountain and prairie regions have the shortest lags, 9 and 10 days, respectively (Table 1). The coast and Mediterranean California sites have the greatest lags (27 days). Figure 6 demonstrates that the regional differences in lag are spatially coherent. Almost all of the prairie and mountain sites have low lag values. Similarly, nearly all of the coast and Mediterranean California sites have high lag values. (Insert Figure 6 here).

When allowing for site-specific lags, the average R^2 value for the correlation between NMRI and NDVI increases from 0.31 (no lag) to 0.53 (Table 1). In general, the gain in R^2 due to introducing lags is similar from region-to-region, from 0.16 in the mountain region to 0.26 in the Mediterranean California region (Figure 5). Thus, the highest and lowest R^2 values including lags are in the prairie and coast regions (0.72 ± 0.1 and 0.28 ± 0.2, respectively) (Table 1, Figure 6(*a*)). Overall, R^2 values and lag times are inversely correlated (Figure 6): maximum R^2 values

are highest in the prairies and mountains where lag days are the least. Minimum R^2 are in the coast regions where lag days are the most.

3.3 Relationship between NMRI and NDVI phenology metrics

Phenology metric results are presented in Table 2 and Figure 7. (Insert Table 2 and Figure 7 here). Figure 7 shows the start of season (SOS) date determined using NDVI and NMRI, for each site and for each year separately. SOS determined using NMRI is later or similar to NDVI, but almost never earlier. This is consistent with the lag results presented above. On average, NDVI SOS precedes that of NMRI by 50 days (Table 2), but significant regional differences exist. NMRI SOS varies across the western U.S. as expected given temperature and precipitation controls. SOS is earliest for Mediterranean California sites and latest for mountain prairie sites (Table 2, Figure 8*a*). At Mediterranean California sites, NDVI SOS is nearly 60 days earlier than NMRI SOS. In contrast, NDVI SOS from prairie sites is only 15 days earlier than determined from NMRI (Table 2). In almost all cases, the NDVI-NMRI difference in SOS is greater than the lag which yields the greatest correlation, by a factor of nearly two. This is the case because SOS depends only on timing of growth. In contrast, the calculated lag depends on both the timing of growth and senescence, the latter which tends to be similar between NDVI and NMRI. (Insert Figure 8 here).

Season length results are similar to SOS results (not shown). Season length is longer when determined from NDVI than from NMRI, 169 days compared to 133 days when averaged across all sites (Table 2). The greatest differences in season length by region are for coast and Mediterranean California sites. The smallest differences are for desert and mountain sites.

The peak vegetation dates determined from NMRI and NDVI are generally correlated (R^2=0.43) (Figure 7*b*). Averaged over all sites, peak day determined from NMRI is later by 31

days (Table 2). By region, NMRI-NDVI peak day differences are greatest for Mediterranean California sites (36 days) and least for mountain sites (9 days) (Figure 8*b* and Table 2). Peak day determined from NMRI varies consistently across the western U.S (Figure 8*c*). Sites in central California peak earliest, followed by sites along the coast, and then sites in the prairies and mountains. Peak vegetation date is most variable within the desert region, possibly because these sites vary greatly in temperature limitations depending upon latitude. NMRI-NDVI differences in peak day also vary across the western U.S. (Figure 8*d*). The greatest differences exist along the coast and for some of the desert sites.

In summary, phenology metrics extracted from the microwave NMRI record have a later start of season, later peak day of year, and shorter season length than determined from optical NDVI data.

3.4 NMRI and NDVI seasonality metrics as a function of climatic variables

The effects of climate parameters on NMRI and NDVI SOS and peak doy are compared in Figure 9 and statistics are presented in Table 3. (Insert Table 3 and Figure 9 here). Mean annual temperature (MAT, ºC) and peak doy are strongly correlated, using either NMRI (R^2=0.59) or NDVI data (R^2=0.45) (Figure 9*c* and *d*). The relationship is negative and approximately linear: as MAT decreases peak doy increases, with NMRI doy occurring slightly after NDVI peak doy. The link between MAT and SOS is not as strong for both indices (R^2=0.26 and 0.30, for NMRI and NDVI respectively) (Table 3). As MAT decreases, NMRI SOS tends to increase. Season length and MAT are not significantly correlated, using either the microwave or the optical dataset. The relationships between Mean Annual Precipitation (MAP, mm) and phenology metrics are not as strong as those using MAT. The only exception is that

season length tends to increase with MAP. The season length-MAP relationship is stronger using NDVI data than NMRI data (Table 3).

4. Discussion

The comparison of NMRI and NDVI data from 184 sites in the western U.S yields the following basic: the start of season is earlier and the growing season is longer according to optical NDVI data than determined from microwave NMRI data. This result is supported by the correlation lag analysis: the correlation between NDVI and NMRI is much stronger when NMRI data is lagged. For both phenology metrics and correlation lag analysis, there are measurable regional differences between the timing of vegetation growth based on NDVI and NMRI. The greatest differences between the timing of seasonal growth cycles recorded by NDVI and NMRI are in Mediterranean California, where NDVI SOS is nearly 60 days earlier. In comparison, NDVI and NMRI fluctuations are more closely synchronized in the prairie and mountains regions, where differences are only ~10 days.

This general result is consistent with the following conceptual model. Initial greening of leaves and the onset of photosynthetic activity yields an increase in NDVI. NMRI is not affected by greenup because this microwave index is sensitive to vegetation water content. Photosynthetic activity and the resulting growth of leaves and stalks yield higher vegetation water content, which leads to an increase in NMRI. The lag between greenup and increased vegetation water content is greatest in the Mediterranean California region. In this area, wintertime precipitation yields greenup of vegetation following seasonal drought. However, peak biomass and vegetation water content are observed approximately two months later. In the prairie and mountains region, the greenup and increase in vegetation water content are more

synchronized, as both occur in response to warming temperatures during springtime. We now discuss these regional differences in more detail.

The prairie and mountain region sites, as well as some desert sites, are located in regions with strong temperature limitations on vegetation growth (Nemani et al., 2003). Sites of this variety are located in Montana, eastern Washington, eastern Oregon, and Idaho. NMRI and NDVI amplitude values are intermediate. These sites have the highest R^2 correlation values between NMRI and NDVI, and the correlation improves with lags of 9 to 15 days. Phenology metrics calculated from NDVI yield a slightly earlier SOS and peak doy compared to those from NMRI. These differences are small compared to other regions.

In these areas, low winter temperatures prevent vegetation growth until there is an increase in soil and air temperatures during spring (Nemani et al., 2003). Our phenology results suggest that in these temperature-limited regions greenup and increases in vegetation water content are largely synchronous, and occur later in the season than in regions constrained by insolation or precipitation. This result could be biased by the location of PBO sites in the region, which are located nearly exclusively in areas dominated by grasses.

Temperature-limitations are not important in the Mediterranean California region compared to the controls related to seasonal variations in precipitation. These sites have high NMRI and high NDVI seasonal amplitudes. The correlation between NDVI and NMRI is relatively low, particularly near the coast. This is the case due to the nearly two month delay between early season increases in NDVI and NMRI. The correlation increases to maximum values with lags of ~30 days. In seasonally-arid ecosystems, activation of photosynthetic material and resultant greening occurs rapidly after initial precipitation events. Based on the

NMRI records, the resulting increases in vegetation water content require ~2 months of photosynthetic activity and plant growth.

Water limitations are even greater in the desert region, including sites in Nevada, eastern California, western Utah, and southern Idaho. These sites have low NMRI and NDVI seasonal amplitude signals. The correlation between NMRI and NDVI is low, at least partly due to the small seasonal vegetation signals at these sites. Minimal vegetation growth yields noisy, low amplitude signals, which minimize the utility of both the calculated phenology metrics and the correlation results.

Comparison of NMRI and NDVI from the northwest coastal region yielded problematic results. First, the coastal region sites have intermediate seasonal NDVI amplitudes but the lowest NMRI amplitudes. The correlation between NMRI and NDVI was very low compared to the other regions, both without and with inclusion of lags. We explain these results as follows. In the coast region, the NDVI signal is partially affected by forested areas within the sampling footprint. In forested areas, PBO GPS sites are located in clearings to minimize multipath from tall vegetation. Thus, the NMRI signal is sensitive to the grasses, shrubs and small trees that dominate these clearings. The large and unexpected differences between NMRI and NDVI records from the coast region likely indicate differences in the sampling footprints of the two remote sensing approaches, not differences between NMRI and NDVI from the same vegetation. Therefore, care must be taken when using NMRI records to evaluate the scale at which the measurements are representative.

5. Conclusions

The microwave scattering index NMRI exhibits a seasonal cycle that is consistent with vegetation growth and senescence in non-forested ecosystems. Phenology determined from

NMRI varies across the western U.S. in a fashion that is consistent with climate constraints. In locations with relatively high temperatures and cold-season precipitation, the start of season and timing of peak vegetation growth occur in winter and early spring, respectively. In contrast, the start of season in prairie and mountain sites occurs in late spring and peak growth is observed during the summer.

The seasonal fluctuations in NMRI are consistent with those observed from NDVI, but clear differences exist at the regional scale. The correlation between the two indices is lowest for Mediterranean California and coast sites and highest for mountain and prairie sites. The correlation increases at all sites once NMRI is lagged relative to NDVI, with the duration of lag varying by region. Using NMRI, there is a later start of season, later peak day of year, and shorter season length. The observed differences between NMRI and NDVI are expected because the two indices are sensitive to different aspects of vegetation. Thus, phenologic information extracted from the microwave-based NMRI complements analyses based on optical indices such as NDVI.

References

Al-Bakri, J.T, and J.C Taylor. 2003. "Application of NOAA AVHRR for Monitoring Vegetation Conditions and Biomass in Jordan." *Journal of Arid Environments* 54 (3) (July): 579–593. doi:10.1006/jare.2002.1081.

De Beurs, K. M. 2008. "Lecture 2: Modeling of Land Surface Phenology with Satellite Imagery." In *Madison LSP Workshop*.

Box, E. O., B. N. Holben, and V. Kalb. 1989. "Accuracy of the AVHRR Vegetation Index as a Predictor of Biomass, Primary Productivity and Net CO2 Flux." *Vegetatio* 80 (2) (June): 71–89. doi:10.1007/BF00048034.

Brakke, T.W., E.T. Kanemasu, and J.L. Steiner. 1981. "Microwave Radar Response to Canopy Moisture, Leaf-area Index, and Dry Weight of Wheat, Corn, and Sorghum." *Remote Sensing of Environment* 220: 207–220.

Burke, I .C., T. G. F. Kittel, W. K. Lauenroth, P Snook, C. M. Yonker, and W. J. Parton. 1991. "Regional Analysis of Great the Central Plains Sensitivity to Climate Variability." *Bioscience* 41 (10): 685–692.

Champion, I., and G. Guyot. 1993. "Estimating Surface Soil Moisture and Leaf Area Index of a Wheat Canopy Using a Dual-Frequency (C and X Bands) Scatterometer." *Remote Sensing of Environment* 339 (March): 331–339.

Chen, D., J. Huang, and T. J. Jackson. 2005. "Vegetation Water Content Estimation for Corn and Soybeans Using Spectral Indices Derived from MODIS Near- and Short-wave Infrared Bands." *Remote Sensing of Environment* 98 (2-3) (October): 225–236. doi:10.1016/j.rse.2005.07.008.

Cihlar, J., L. St-Laurent, and J.A. Dyer. 1991. "Relation Between the Normalized Difference Vegetation Index and Ecological Variables." *Remote Sensing of Environment* 298 (June 1990): 279–298.

Cleland, E. E., I. Chuine, A. Menzel, H. Mooney, and M. D. Schwartz. 2007. "Shifting Plant Phenology in Response to Global Change." *Trends in Ecology & Evolution* 22 (7) (July): 357–65. doi:10.1016/j.tree.2007.04.003.

Eidenshink, J. 1992. "The 1990 Conterminous US AVHRR Data Set." *Photogrammetric Engineering and Remote Sensing* 58 (March 1990).

Fischer, A. 1994. "A Model for the Seasonal Variations of Vegetation Indices in Coarse Resolution Data and Its Inversion to Extract Crop Parameters." *Remote Sensing of Environment* 230 (October 1991): 220–230.

Gamon, J. A., C. B. Field, M. L. Goulden, K. L. Griffin, E. Hartley, G. Joel, J. Peñuelas, and R. Valentini. 2012. "Relationship Between NDVI, Canopy Structure, and Photosynthesis in Three Californian Vegetation Types." *Ecological Applications* 5 (1): 28–41.

Gao, B. 1996. "NDWI A Normalized Difference Water Index for Remote Sensing of Vegetation Liquid Water From Space" 266 (April 1995): 257–266.

Goetz, S. J. 1997. "Multi-sensor Analysis of NDVI , Surface Temperature and Biophysical." *International Journal of Remote Sensing* 18 (1): 71–94.

Hargrove, W. W., and F.M. Hoffman. 1999. "Using Multivariate Clustering to Charactreize Ecoregion Border." *Computing in Sceince and Engineering*: 18–25.

Hobbs, R.J., S. Yates, and H.A. Mooney. 2007. "Long-term Data Reveal Complex Dynamics in Grassland in Relation to Climate and Disturbance." *Ecological Monographs* 77 (4): 545–568.

Holm, A. 2003. "The Use of Time-integrated NOAA NDVI Data and Rainfall to Assess Landscape Degradation in the Arid Shrubland of Western Australia." *Remote Sensing of Environment* 85 (2) (May 15): 145–158. doi:10.1016/S0034-4257(02)00199-2.

Huete, A.R. 1988. "A Soil-adjusted Vegetation Index (SAVI)." *Remote Sensing of Environment* 309: 295–309.

Jones, M. O., L. A. Jones, J. S. Kimball, and K. C. McDonald. 2011. "Satellite Passive Microwave Remote Sensing for Monitoring Global Land Surface Phenology." *Remote Sensing of Environment* 115 (4) (April 15): 1102–1114. doi:10.1016/j.rse.2010.12.015.

Jones, M. O., J. S. Kimball, L. A. Jones, and K. C. McDonald. 2012. "Satellite Passive Microwave Detection of North America Start of Season." *Remote Sensing of Environment* 123 (August): 324–333. doi:10.1016/j.rse.2012.03.025.

Jönsson, P., and L. Eklundh. 2004. "TIMESAT—a Program for Analyzing Time-series of Satellite Sensor Data." *Computers & Geosciences* 30 (8) (October): 833–845. doi:10.1016/j.cageo.2004.05.006.

Karl, T.R., B.E. Gleason, M.J. Menne, J.R. McMahon, R.R. Heim Jr., M.J. Brewer, K.E. Kunkel, et al. 2012. "U . S . Temperature and Drought : Recent Anomalies and Trends." *Eos, Transactions American Geophysical Union* 93 (47): 2011–2013.

Kim, Y., T. Jackson, and R. Bindlish. 2012. "Radar Vegetation Index for Estimating the Vegetation Water Content of Rice and Soybean." *IEEE Geoscience and Remote Sensing Letters* 9 (4): 564–568.

Larson, K. M., E. E. Small, E. D. Gutmann, A. L. Bilich, J. J. Braun, and V.U. Zavorotny. 2008. "Use of GPS Receivers as a Soil Moisture Network for Water Cycle Studies." *Geophysical Research Letters* 35 (24) (December 24): L24405. doi:10.1029/2008GL036013.

Larson, K.M. and E.E. Small, Normalized Microwave Reflection Index, part 1: A Vegetation Measurement Derived from GPS Data, *IEEE JSTARS*, in review, available at http://spot.colorado.edu/~kristine/Kristine_Larson/Publications.html

Loveland, T. R., B. C. Reed, J.F. Brown, D.O. Ohlen, Z. Zhu, L. Yang, and J.W. Merchant. 2000. "Development of a Global Land Cover Characteristics Database and IGBP DISCover from 1 Km AVHRR Data." *International Journal of Remote Sensing* 21 (6): 1303–1330.

Lu, D. 2006. "The Potential and Challenge of Remote Sensing Based Biomass Estimation." *International Journal of Remote Sensing* 27 (7) (April): 1297–1328. doi:10.1080/01431160500486732.

Mitchell, K.E., D. Lohmann, P.R. Houser, E.F. Wood, J.C. Schaake, A. Robock, B.A. Cosgrove, et al. 2003. "The Multi-institution North American Land Data Assimilation System (NLDAS): Utilizing Multiple GCIP Products and Partners in a Continental Distributed Hydrological Modeling System." *J. Geophysical Research- Atmosphere*.

Montandon, L., and E. Small. 2008. "The Impact of Soil Reflectance on the Quantification of the Green Vegetation Fraction from NDVI." *Remote Sensing of Environment* 112 (4) (April 15): 1835–1845. doi:10.1016/j.rse.2007.09.007.

Morisette, J.T., A. D. Richardson, A. K. Knapp, J.I. Fisher, E. Graham, J. A., B.E. Wilson, et al. 2009. "Tracking the Rhythm of the Seasons in the Face of Global Change: Phenological Research in the 21st Century." *Frontiers in Ecology and the Environment* 7 (5) (June): 253–260. doi:10.1890/070217.

Myneni, R. B., and D. L. Williams. 1994. "On the Relationship Between FAPAR and NDVI." *Remote Sensing of Environment* 211 (April): 200–211.

Nemani, R. R., C. D. Keeling, H. Hashimoto, W.M. Jolly, S. C. Piper, C. J. Tucker, R. B. Myneni, and S. W. Running. 2003. "Climate-driven Increases in Global Terrestrial Net Primary Production from 1982 to 1999." *Science* 300 (5625) (June 6): 1560–3. doi:10.1126/science.1082750.

Omernik, J. M. 1987. "Ecoregions of the Conterminous United States." *Annals of The Association of American Geographers* 77 (1): 118–125.

O'Neill, P.E., T.J. Jackson, B.J. Blanchard, J.R. Wang, and W.I. Gould. 1984. "Effects of Corn Stalk Orientation and Water Content on Passive Microwave Sensing of Soil Moisture." *Remote Sensing of Environment* 16 (1) (August): 55–67. doi:10.1016/0034-4257(84)90027-0.

Parmesan, C. 2007. “Influences of Species, Latitudes and Methodologies on Estimates of Phenological Response to Global Warming.” *Global Change Biology* 13 (9) (September): 1860–1872. doi:10.1111/j.1365-2486.2007.01404.x.

Paruelo, J.M., and M.R. Aguiar. 1993. “Environmental Controls of NDVI Dynamics in Patagonia Based on NOAA-AVHRR Satellite Data.” *Journal of Vegetation Science* 4: 425–428.

Paruelo, J.M., H.E. Epstein, W.K. Lauenroth, and I.C. Burke. 1997. “ANPP Estimates from NDVI for the Central Grassland Region of the United States.” *Ecology* 78 (3): 953–958.

Paruelo, J.M., and W.K. Lauenroth. 1995. “Regional Patterns of Normalized Difference Vegetation Index in North American Shrublands and Grasslands.” *Ecology* 76 (6): 1888–1898.

Peñuelas, J. 2009. “Phenology Feedbacks on Climate Change.” *Science* 324 (5929) (May 15): 887–8. doi:10.1126/science.1173004.

Rodriguez-Iturbe, I. 2000. “Ecohydrology : A Hydrologic Perspective of Climate-soil-vegetation Dynamics.” *Water Resources Research* 36 (1): 3–9.

Rondeaux, G., M. Steven, and F. Baret. 1996. “Optimization of Soil-Adjusted Vegetation Indices.” *Remote Sensing of Environment* 107 (August 1994): 95–107.

De Roo, R.D., F.T. Ulaby, and M.C. Dobson. 2001. “A Semi-empirical Backscattering Model at L-band and C-band for a Soybean Canopy with Soil Moisture Inversion.” *IEEE Transactions on Geoscience and Remote Sensing* 39 (4) (April): 864–872. doi:10.1109/36.917912.

Running, S.W., and R.R. Nemani. 1988. “Relating Seasonal Patterns of the AVHRR Vegetation Index to Simulated Photosynthesis and Transpiration of Forests in Different Climates.” *Remote Sensing of Environment* 24: 347–367.

Schmugge, T. 1978. “Remote Sensing of Surface Soil Moisture.” *Journal of Applied Meteorology* 17: 1549–1557.

Schwartz, M.D., R. Ahas, and A. Aasa. 2006. “Onset of Spring Starting Earlier Across the Northern Hemisphere.” *Global Change Biology* 12 (2) (February): 343–351. doi:10.1111/j.1365-2486.2005.01097.x.

Sellers, P.J., J.A. Berry, G.J. Collatz, C.B. Field, and F.G. Hall. 1992. “Canopy Reflectance, Photosynthesis, and Transpiration. III. A Reanalysis Using Improved Leaf Models and a New Canopy Integration Scheme.” *Remote Sensing of Environment* 42 (3) (December): 187–216. doi:10.1016/0034-4257(92)90102-P.

Sellers, P.J., M.D. Heiser, and F.G. Hall. 1995. "Effects of Spatial Variability in Topography, Vegetation Cover and Soil Moisture on Area-averaged Surface Fluxes: A Case Study Using the FIFE 1989 Data." *Journal of Geophysical Research* 100 (95).

Serrano, L., I. Filella, and J. Penuelas. 2000. "Remote Sensing of Biomass and Yield of Winter Wheat Under Different Nitrogen Supplies." *Crop Science*: 723–731.

Small, E. E., K. M. Larson, and J.J. Braun. 2010. "Sensing Vegetation Growth with Reflected GPS Signals." *Geophysical Research Letters* 37 (12) (June 16): L12401. doi:10.1029/2010GL042951.

Small, E.E., K.M. Larson, and W. Smith, Normalized Microwave Reflection Index, part 2: Validation of Vegetation Water Content Estimates at Montana Grasslands, *IEEE JSTARS*, in review, available at http://spot.colorado.edu/~kristine/Kristine_Larson/Publications.html.

Swets, D. L., Augustana College, S Summit Ave, and Sioux Falls. 2001. "A Weighted Least-Squares Approach to Temporal NDVI Smoothing" (Figure 1).

Tarpley, J.D., S.R. Schneider, and R.L. Money. 1984. "Global Vegetation Indices from the NOAA-7 Meteorological Satellite." *Journal of Climate and Applied Meterology* 23: 491–494.

U.S. EPA (Environmental Protection Agency). 2011. Landscape and predictive tools: a guide to spatial analysis for environmental assessment. Risk Assessment Forum. Washington, DC. EPA/100/R-11/002.

Ulaby, F.T., C.T. Allen, G. Eger, and E. Kanemasu. 1984. "Relating the Microwave Backscattering Coefficient to Leaf Area Index." *Remote Sensing of Environment*.

Ulaby, F.T., and E.A. Wilson. 1985. "Microwave Attenuation Properties of Vegetation Canopies." *IEEE Transactions on Geoscience and Remote Sensing* (5): 746–753.

Wang, J., P. M. Rich, and K. P. Price. 2003. "Temporal Responses of NDVI to Precipitation and Temperature in the Central Great Plains, USA." *International Journal of Remote Sensing* 24 (11) (January): 2345–2364. doi:10.1080/01431160210154812.

White, M. A. 2005. "A Global Framework for Monitoring Phenological Responses to Climate Change." *Geophysical Research Letters* 32 (4): 2–5. doi:10.1029/2004GL021961.

White, M. A., K. M. De Beurs, K. Didan, D. W. Inouye, A. D. Richardson, O. P. Jensen, J. O'Keefe, et al. 2009. "Intercomparison, Interpretation, and Assessment of Spring Phenology in North America Estimated from Remote Sensing for 1982-2006." *Global Change Biology* 15 (10) (October): 2335–2359. doi:10.1111/j.1365-2486.2009.01910.x.

Wiken, Ed, Francisco Jiménez Nava, and Glenn Griffith. 2011. North American Terrestrial Ecoregions—Level III. Commission for Environmental Cooperation, Montreal,Canada.

Wolfe, D.W., M.D. Schwartz, and A.N. Lakso. 2005. “Climate Change and Shifts in Spring Phenology of Three Horticultural Woody Perennials in Northeastern USA.” *International Journal of Biometeorol* 49: 303–309. doi:10.1007/s00484-004-0248-9.

Region Name	Population Size	NMRI Mean Range	NDVI Mean Range	Mean R^2	Max. Mean R^2	Lag Days
Average (2008-2012)	184	0.15±0.07	0.32±0.11	0.31±0.21	0.53±0.20	21±13
Mountain	25	0.14±0.06	0.35±0.10	0.46±0.18	0.61±0.23	9±7
Coast	14	0.10±0.03	0.30±0.05	0.10±0.14	0.28±0.16	26±16
Prairie	8	0.13±0.03	0.32±0.09	0.49±0.14	0.72±0.07	10±6
Desert	38	0.11±0.06	0.19±0.10	0.37±0.21	0.54±0.21	15±9
Med. CA	99	0.18±0.07	0.36±0.09	0.26±0.18	0.52±0.17	27±11
Grassland	*66*	*0.20±0.07*	*0.39±0.09*	*0.27±0.17*	*0.54±0.17*	*28±11*
Shrubs	*33*	*0.13±0.05*	*0.31±0.08*	*0.24±0.18*	*0.48±0.15*	*25±12*

Table 1. Mean NMRI and NDVI parameters by region. Mediterranean California has been further subdivided into grassland and shrub sites.

2008-2012	**SOS (doy)**	**Season Length (days)**	**Peak Doy**
NDVI Average	18	169	111
NMRI Average	68	133	142
Mountain (n=22)			
NDVI	87	138	169
NMRI	121	121	178
Coast (n=14)			
NDVI	4	233	135
NMRI	96	131	172
Prairie (n=8)			
NDVI	110	128	175
NMRI	125	103	187
Desert (n=30)			
NDVI	51	142	135
NMRI	82	125	162
Mediterranean California (n=99)			
NDVI	-15	179	82
NMRI	43	138	118
Grasslands (n=66)			
NDVI	-12	177	82
NMRI	43	134	117
Shrubs (n=33)			
NDVI	-21	182	82
NMRI	42	145	120

Table 2. Phenology metrics extracted for NDVI and NMRI. Overall NMRI has a later SOS, later peak doy, and shorter season length. Mediterranean California sites are subdivided into grasslands and shrubs.

Climate Variable	Phenology Metric	Index	R^2	p-value
Mean Annual Temperature	SOS	NMRI	0.26	0.00
		NDVI	0.30	0.00
	Season Length	NMRI	0.00	0.23
		NDVI	0.00	0.21
	Peak doy	NMRI	0.59	0.00
		NDVI	0.45	0.00
Mean Annual Precipitation	SOS	NMRI	0.01	0.05
		NDVI	0.01	0.04
	Season Length	NMRI	0.09	0.00
		NDVI	0.29	0.00
	Peak doy	NMRI	0.08	0.00
		NDVI	0.02	0.00

Table 3. Phenology correlation and p-values, $p \leq 0.05$ for R^2 to be significant (n=865).

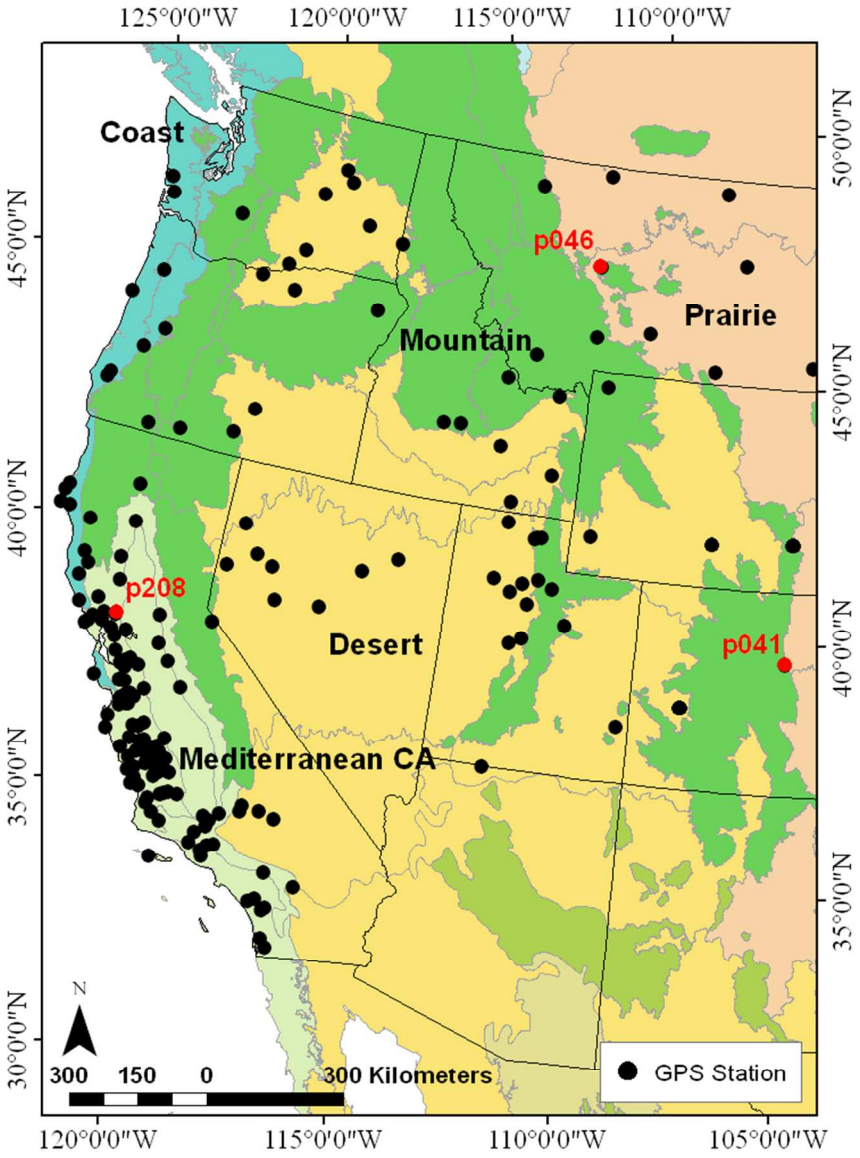

Figure 1. Map showing location of GPS stations used in this study. Three sites discussed in the text are highlighted in red. The five regions are colored and labeled in black text.

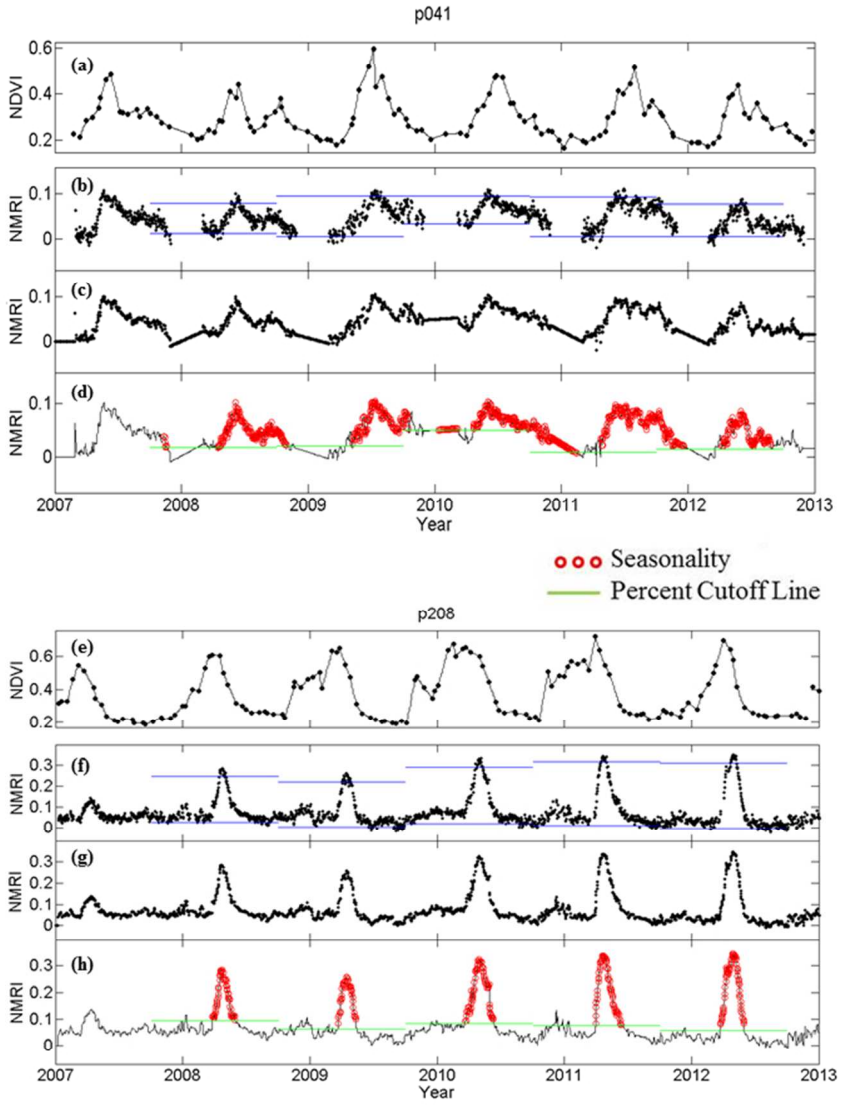

Figure 2. Time series examples for sites p041 (CO) and p208 (CA). (*a*) and (*e*): NDVI data, including linear interpolation between observed values. NDVI Phenology metrics are calculated from the interpolated data. (*b*) and (*f*): NMRI after removal of data on days with snow and heavy precipitation. Blue lines show 95th and 5th percentile cutoffs for amplitude calculation, determined separately for each water year. (*c*) and (*g*): NMRI time series after application of a five-day centered median filter. (*d*) and (*h*): Application of phenology analysis to NMRI time series. Green line is 25% cutoff value, which varies by year. Red shows the interval above the 25% cutoff with duration greater than 40 days.

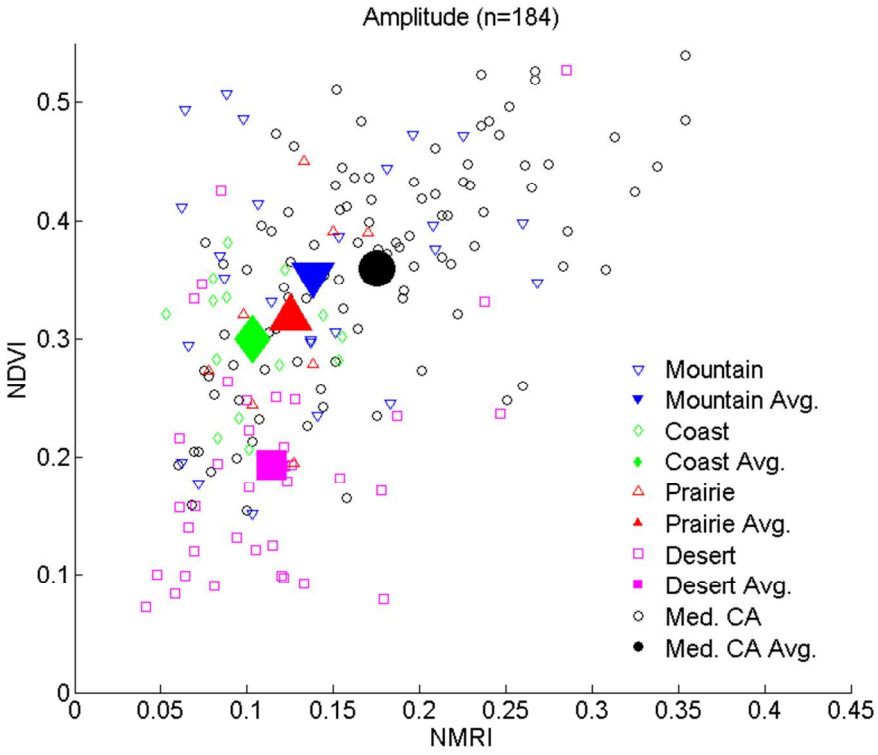

Figure 3. NMRI and NDVI average amplitude for 2008-2012 data series. Each point represents one of 184 sample sites. Filled are averages for each region (see Table 1).

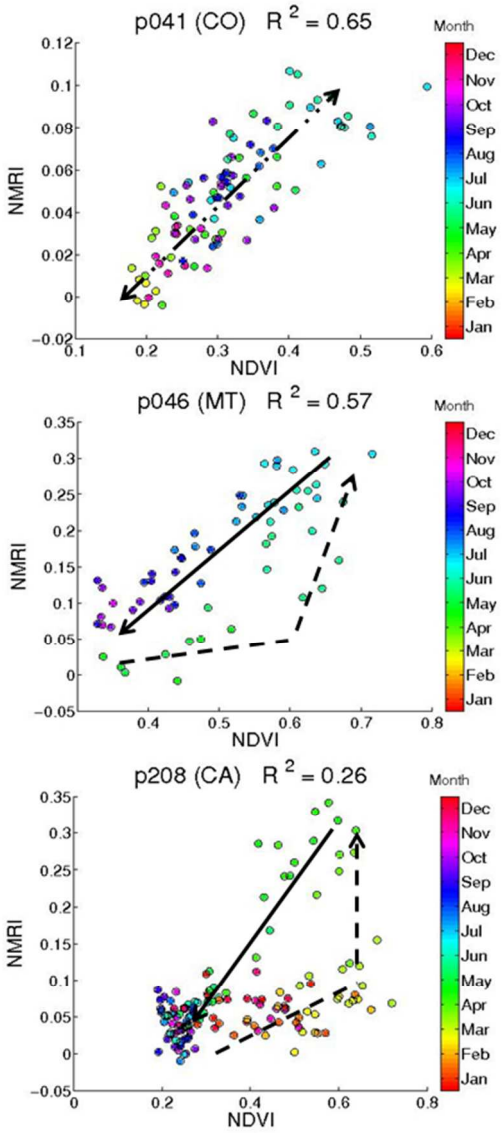

Figure 4. NMRI-NDVI scatterplots for p041 (CA), p046 (MT), and p208 (CA). Each point represents one NDVI sample day on which NMRI data has also been extracted for 2007-2012. Colors indicate date of observation. Dashed lines represent vegetation greenup and increasing in water content while solid lines illustrate vegetation decline following senescence.

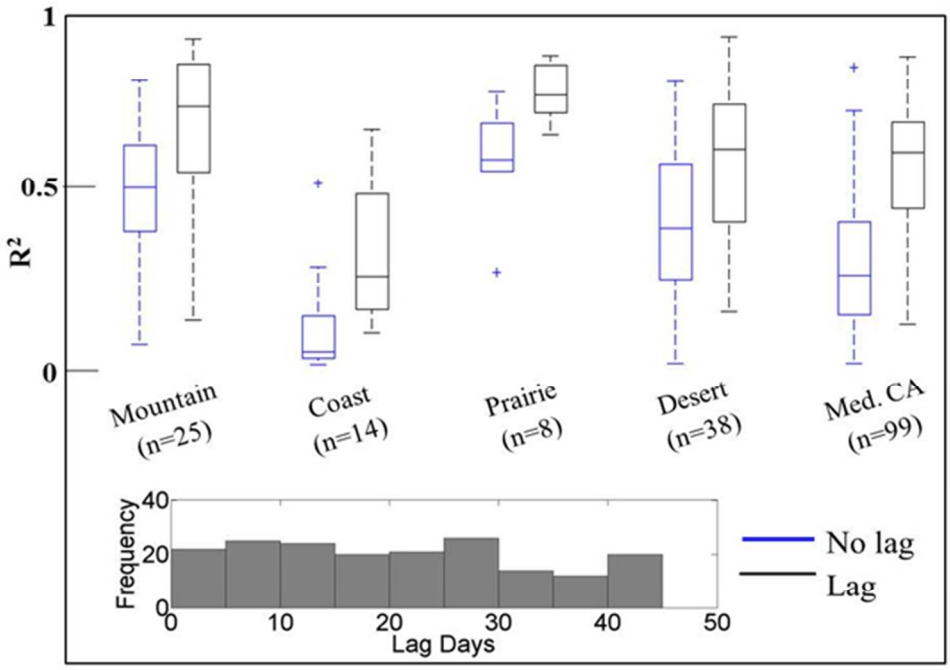

Figure 5. NDVI-NMRI correlations grouped by region. For each region, correlations without lag are in blue and with lags are in black. Plot displays outliers (+), median, quartiles, maximum, and minimum values. Inset histogram shows number of days that yield the maximum correlation. The highest lag days (>40 days) are found at coastal sites, both in the coast and Mediterranean California regions.

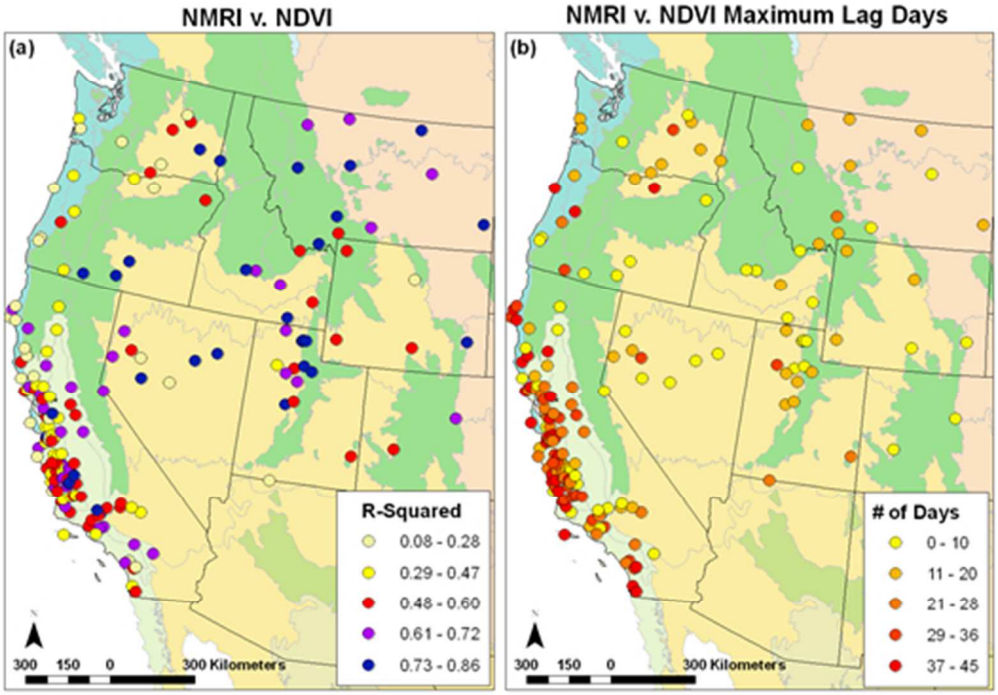

Figure 6. The left panel shows R^2 values with lags that yield the greatest correlation, the mean is 0.53. The right panel displays the number of lag days that yields the strongest correlation

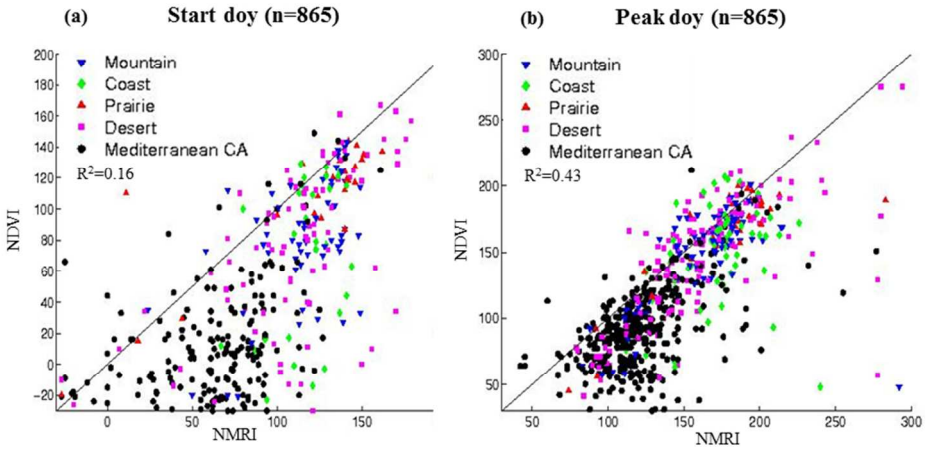

Figure 7. SOS doy and peak vegetation doy determined from NDVI and NMRI. The one-to-one line is displayed. Color indicates region. Each point represents one water-year of data for one site (173 sites for 5 water-years, for 865 total points).

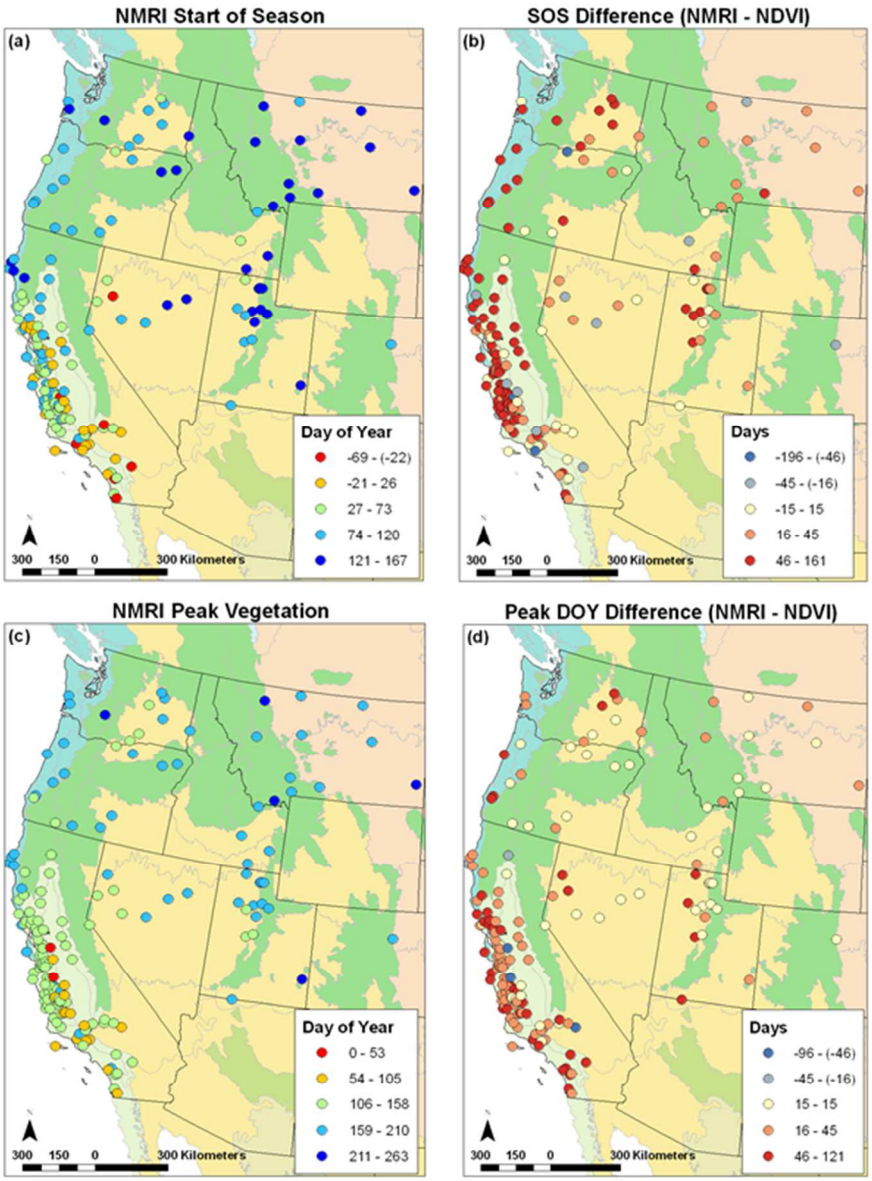

Figure 8. Phenology metrics determined from NMRI and differences between metrics determined from NMRI and NDVI: (*a*) Start of season (SOS) doy from NMRI; (*b*) difference in SOS doy (NMRI minus NDVI), positive numbers indicate later NMRI SOS doy than NDVI; (*c*) peak vegetation doy from NMRI; (*d*) difference in peak doy (NMRI-NDVI).

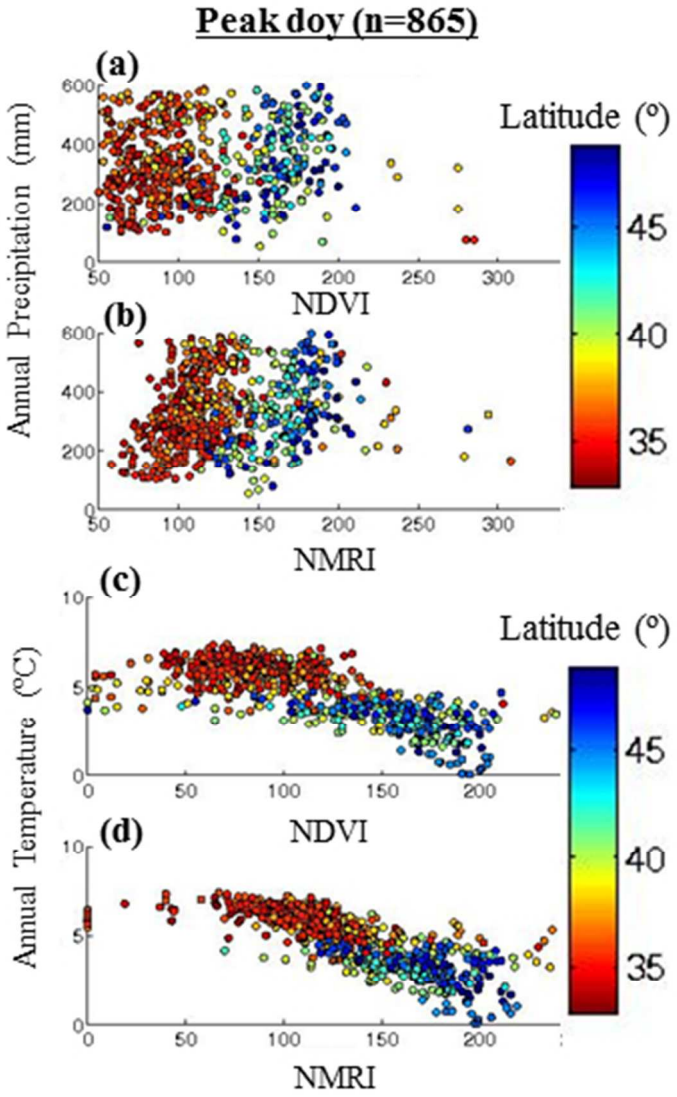

Figure 9. Peak vegetation doy (*a*-*d*) organized by mean annual precipitation (*a* and *b*) and mean annual temperature (*c* and *d*) and NMRI (*b* and *d*) or NDVI (*a* and *c*) and stratified by latitude. Each point (n=865) represents one water-year of data for one site (2008-2012).